NJC

PAPER

View Article Online
View Journal | View Issue

Cite this: *New J. Chem.*, 2015, 39, 8673

New insights into metal ion–crown ether complexes revealed by SEIRA spectroscopy†

Yoshiya Inokuchi,*[a] Takayuki Ebata,[a] Toshiaki Ikeda,[a] Takeharu Haino,[a] Tetsunari Kimura,[b] Hao Guo[b] and Yuji Furutani[b]

We demonstrate a powerful spectroscopic technique, surface-enhanced infrared absorption (SEIRA) spectroscopy, not only for detecting host–guest complexes in solution but also for examining the relationship between the guest selectivity, complex structure, and solvent effect. We synthesize thiol derivatives of 15-crown-5 and 18-crown-6 [2-(6-mercaptohexyloxy)methyl-15-crown-5 (15C5-C_1OC_6-SH) and 2-(6-mercaptohexyloxy)methyl-18-crown-6 (18C6-C_1OC_6-SH)], which are adsorbed on gold surfaces through S–Au bonds. The IR difference spectra of the M^+·15C5-C_1OC_6 (M = Li, Na, K, Rb, and Cs) complexes on gold are observed using aqueous solutions of MCl by SEIRA spectroscopy. The spectra show a noticeable change in the C–O stretching vibration at around 1100 cm^{-1}. The spectral patterns of M^+·15C5-C_1OC_6 are similar for Li^+ and Na^+, and for K^+, Rb^+, and Cs^+; the interaction between the metal ions and 15C5-C_1OC_6 changes drastically between Na^+ and K^+ in the series of alkali metal ions. On the other hand, the equilibrium constant for complex formation determined by the IR intensity shows clear preference for Na^+ ions. We also observe the IR difference spectra of M^+·18C6-C_1OC_6 in methanol and compare them with those in water. The spectral patterns in methanol are almost the same as those in water, but the equilibrium constant in methanol does not show preference for any ion, different from the K^+ preference in water. From these findings we attribute the origin of the ion selectivity of 15C5 and 18C6 in solution to the interaction between the metal ions and the crown ethers in the complexes or the solvation energy of free ions. In the case of 15C5-C_1OC_6 in water, the preference of Na^+ over K^+, Rb^+, and Cs^+ can be attributed to the strength of the interaction or the size matching between metal ions and 15C5-C_1OC_6; the Na^+ selectivity over Li^+ ions is dominated by the solvation energy of free ions. For 18C6-C_1OC_6 in methanol, the equilibrium constant for complex formation becomes much bigger in methanol than that in water and loses the selectivity in methanol, because the solvation energy in methanol is fairly smaller than that in water, predominating the contribution from the strength of the interaction between metal ions and 18C6-C_1OC_6. The IR spectra measured by SEIRA spectroscopy are quite sensitive to properties of host–guest complexes such as the intermolecular interaction, the structure, and the orientation against the gold surface. However, the evidence for guest selectivity emerges primarily in the intensity of the spectra, rather than band positions or spectral patterns in the IR spectra.

Received (in Victoria, Australia) 11th July 2015,
Accepted 26th August 2015

DOI: 10.1039/c5nj01787d

www.rsc.org/njc

1. Introduction

In this study, we investigate the IR spectroscopy of alkali metal ion–crown ether complexes on gold; crown ethers are bound to gold through S–Au bonds, and solutions of alkali chloride salts are placed on them for the complexes to be formed. Host molecules such as crown ethers (CEs) hold guest ions selectively.[1] For instance, 18-crown-6 (18C6) and 15-crown-5 (15C5) show a high encapsulation efficiency for K^+ and Na^+ ions in solutions, respectively, among alkali metal ions.[1b,c] The preferential capture of guest species has been explained mainly by the size matching with the cavity of host molecules.[2] The crystal structure of host–guest complexes was examined by X-ray diffraction.[1b,3] In crystals, however, counter anions and solvent molecules are also bound to

[a] *Department of Chemistry, Graduate School of Science, Hiroshima University, Higashi-Hiroshima, Hiroshima 739-8526, Japan.*
E-mail: y-inokuchi@hiroshima-u.ac.jp; Tel: +81-82-424-7101
[b] *Institute for Molecular Science, Myodaiji, Okazaki 444-8585, Japan*

† Electronic supplementary information (ESI) available: The IR absorption spectra of the thiol derivatives used in this study (Fig. S1). The proposed orientation of the Rb^+·15C5 component at the interface, and the dipole derivative of the most intense C–O stretching band for Na^+·15C5-C_1OC_6-CH_3 and Rb^+·15C5-C_1OC_6-CH_3 (Fig. S2). The concentration dependence of the peak-to-peak intensity at around 1100 cm^{-1} in the IR difference spectra of the M^+·18C6-C_1OC_6 complexes using the methanol solutions of MCl (Fig. S3). The optimized structures of bare 15C5-C_1OC_6-CH_3 and the M^+·15C5-C_1OC_6-CH_3 (M = Li, Na, K, Rb, and Cs) complexes in water (Fig. S4–S9). See DOI: 10.1039/c5nj01787d

guest cations, which often affects the structure of host–guest complexes. Previous studies of mass spectrometry, UV/IR spectroscopy, and theoretical calculations of host–guest complexes suggested that the solvent is highly involved in the ion selectivity in the liquid phase.[1b,c,4] Therefore, it is necessary to determine the complex structure under solvated or microsolvated conditions to elucidate the origin of the ion selectivity in solutions. Our group has been investigating the structure of alkali metal ion–CE complexes and their hydrated ones in the gas phase by UV photodissociation and IR-UV double resonance spectroscopy.[5] The CE complexes with ionic guests were also studied in the gas phase by IR photodissociation spectroscopy.[6] The complex structure in solutions was examined by using NMR[7] and EXAFS[8] spectroscopy. Vibrational spectroscopy was also performed for CE complexes with guest ions in the condensed phase.[1d,9] The vibrational spectra showed the band shift or broadening, which was attributed to the conformational change of the CEs upon complex formation and fluctuation of the guest position in the crown cavity. In these condensed-phase studies, however, the vibrational spectra were used mainly to detect complex formation and were not analyzed extensively from a perspective of the relationship between the complex structure and the ion selectivity.

More recently, we have obtained the IR spectra of metal ion–CE complexes in solutions by surface-enhanced IR absorption (SEIRA) spectroscopy.[10] In these measurements, CEs are bound to gold surfaces through S–Au chemical bonds, and solutions containing metal ions are placed on the surfaces. We found that the equilibrium constant of 18C6 tagged on the gold surfaces is the largest for K^+ among alkali metal ions. This result is in good agreement with previously reported ones in solutions,[1b,c] showing that this method is well suitable for studying the encapsulation process in solutions. Thanks to the enhancement of the IR absorption by gold surfaces and its confinement to the immediate vicinity of the surfaces,[11] the formation of metal ion–CE complexes can be detected with very high sensitivity, avoiding interference from strong absorption of solvent. The high sensitivity nature of SEIRA spectroscopy also makes it possible to measure the IR spectra with a very wide range of guest concentrations. This will provide the equilibrium constant for the complex formation from the IR spectra and reveal the relationship between the complex structure and the ion selectivity as in the case of a biological sample.[11b,d] Since the encapsulated metal ions can be removed and changed to other ions very easily with the CEs kept on gold surfaces, systematic and prompt measurements of the IR spectra are possible, which is essential for quantitative measurements with a series of metal ions. In this experiment, it is not necessary to dissolve CEs and metal ions in the same solvent. This enables us to study the solvent effect on encapsulation by using a variety of solvents. In addition, the tagging of CEs on gold surfaces is of great advantage for applications such as ion sensing.[12]

In this paper, we examine the crown size and solvent dependence on the complex formation of CEs by SEIRA spectroscopy. We synthesize thiol derivatives of 15C5 and 18C6, which are adsorbed on gold surfaces through S–Au chemical bonds. Two types of solutions, aqueous and methanol solutions of alkali metal chloride salts, are placed on the surface, and IR spectra are measured by SEIRA spectroscopy. We examine the spectral change (frequency shift and intensity change) of 15C5 and 18C6 occurring upon encapsulation of the metal ions. The change in the IR intensity induced by complex formation is dependent on the concentration of metal ions in solutions, which provides the equilibrium constant for complex formation. The results of M^+·15C5 in water and M^+·18C6 in methanol are compared with those of M^+·18C6 in water.[10]

2. Experimental and computational methods

All chemicals for synthesis are purchased and used without further treatment. The synthesis of 2-(6-mercaptohexyloxy)-methyl-15-crown-5 (**1**) and 2-(6-mercaptohexyloxy)methyl-18-crown-6 (**2**) is carried out by following the procedures described in a paper reported by Flink *et al.*[12d] Hereafter these molecules are called 15C5-C_1OC_6-SH and 18C6-C_1OC_6-SH, respectively. Chloride salts of alkali metals are purchased from Wako Pure Chemicals Industries and are dissolved in high-purity water (Millipore) or methanol to prepare aqueous or methanol solutions of alkali metal ions.

We perform SEIRA spectroscopy of CEs tagged on gold surfaces by using a home-made vacuum deposition system and an FTIR spectrometer (Vertex 70, Bruker) coupled with a single reflection Si attenuated total reflection (ATR) system (VeeMAX II, PIKE Technologies). The details of the preparation of gold surfaces on a Si prism have been described in previous studies of Guo *et al.*[13] Briefly, the gold surfaces are formed on an unheated Si crystal by thermal deposition of a gold wire from a tungsten basket in a vacuum chamber with a deposition rate of $\sim$0.005 nm s^{-1}. The thickness of the gold surfaces is $\sim$7 nm, with which the enhancement of IR absorption will be optimum and the distortion of IR spectral features will be minimized.[13] A home-made Teflon chamber is mounted on top of the Si crystal to introduce and retain liquid samples on the gold surfaces. Modification of the gold surfaces with CEs (**1**) or (**2**) is performed by monitoring IR absorption of CEs. A solution of (**1**) or (**2**) dissolved in dimethylsulfoxide (DMSO) with a concentration of $\sim 5 \times 10^{-3}$ M is introduced on gold surfaces. The CEs (**1**) and (**2**) are tagged on the gold surfaces by forming S–Au chemical bonds. We leave the solution of CEs on gold surfaces for 30 minutes for achieving complete coverage of the gold surfaces with CEs. Fig. 1 shows the schematic structure of CEs on gold surfaces. Hereafter the gold surfaces modified with the CEs (**1**) and (**2**) are called 15C5-C_1OC_6 and 18C6-C_1OC_6, respectively. After removing the DMSO solution and washing the surfaces several times with pure water or methanol, FTIR difference spectra are measured repeatedly using solutions of alkali metal chloride salts and pure solvent with a 4 cm^{-1} spectral resolution at room temperature. In every exchange process of metal ions on the same gold surface, we confirm the removal of the metal ions from the gold surface by observing the complete disappearance of the IR bands due to the metal ion–crown ether complexes.

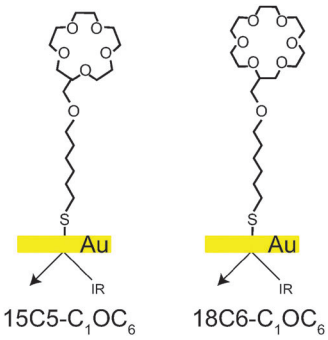

Fig. 1 The structure of the crown ethers chemisorbed on the gold surface.

We calculate the structure and IR spectra of the metal ion complexes of 15C5-C_1OC_6 by terminating the end of the hydrocarbon chain with a CH_3 group.[10] The initial conformational search is performed for the Li^+·15C5-C_1OC_6-CH_3, Na^+·15C5-C_1OC_6-CH_3, K^+·15C5-C_1OC_6-CH_3, and bare 18C6-C_1OC_6-CH_3 under the conditions of water solutions by using the CONFLEX program package and the MMFF94s force field with a search limit of 1 kcal mol^{-1}, which produces more than 1000 conformers.[14] The most stable ~20 conformers found using the force field calculations are then optimized at the M05-2X/6-31+G(d) level with the polarizable continuum model (PCM) of water using the GAUSSIAN09 program package.[15] The CONFLEX program does not include the force field of Rb^+ and Cs^+. For the Rb^+, and Cs^+ complexes, initial forms for the geometry optimization are produced by replacing the K^+ ion in the stable conformers of the K^+·15C5-C_1OC_6-CH_3 complex with Rb^+ or Cs^+ ions. Vibrational analysis is carried out for the optimized structures at the same computational levels. Calculated frequencies at the M05-2X/6-31+G(d) level are scaled with a factor of 0.9389 for comparison with the observed IR spectra.[10] The scaling factor was determined so as to reproduce the C–O stretching vibration of the K^+·18C6-C_1OC_6 complex in water.[10]

3. Results and discussion

3.1. M^+·15C5 and M^+·18C6 in water: cavity size dependence

Fig. 2a–e display the IR difference spectra of M^+·15C5-C_1OC_6 on gold with aqueous solutions of MCl (M = Li, Na, K, Rb, and Cs). These spectra are obtained by subtracting the IR spectrum with pure water from the IR spectra with the aqueous solutions of MCl. The concentration of MCl ranges from 10^{-6} to 1 M for Li and Na and from 10^{-3} to 1 M for K, Rb, and Cs with a sequential step of factors of 10 in concentration; the blue curve in each panel of Fig. 2 shows the spectrum with 1 M. For comparison, the IR difference spectrum of K^+·18C6-C_1OC_6 with an aqueous solution of KCl (100 mM) is shown in Fig. 2f.[10] Broad negative signals appearing above 1200 cm^{-1} at 1 M are due to the bending and libration modes of H_2O in solutions; the introduction of MCl into water deforms the structure of liquid water, showing the broad signal in the difference spectra.[10] Positive and negative sharp signals in Fig. 2 are attributed to the spectral change of the 15C5-C_1OC_6 moiety due to the formation of the M^+·15C5-C_1OC_6 complexes. In all the IR spectra,

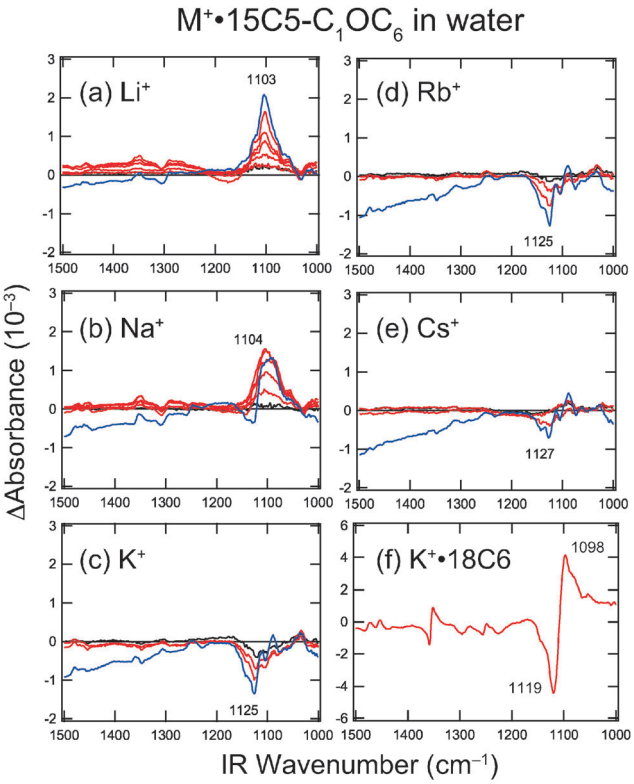

Fig. 2 (a–e) The IR difference spectra of the M^+·15C5-C_1OC_6 (M = Li, Na, K, Rb, and Cs) complexes on the gold surface using aqueous MCl solutions. The concentration of the MCl salts in water ranges from 10^{-6} to 1 M for Li^+ and Na^+ and from 10^{-3} to 1 M for K^+, Rb^+, and Cs^+. The blue curves are the IR difference spectra recorded at 1 M. (f) The IR difference spectrum of the K^+·18C6-C_1OC_6 complex on the gold surface with the aqueous solution of KCl at 100 mM (ref. 10).

noticeable signals are observed at ~1100 cm^{-1}. This frequency corresponds to the C–O stretching vibration;[10] 15C5-C_1OC_6-SH has a strong C–O stretching band at ~1110 cm^{-1}, as shown in Fig. S1 of the ESI.† The spectral features of the IR difference spectra in Fig. 2 are dependent on the metal ions encapsulated. In the spectra of the Li^+ and Na^+ complexes, a positive signal is observed at ~1103 cm^{-1}. In contrast, the IR spectra of the K^+, Rb^+, and Cs^+ complexes show a negative signal at ~1125 cm^{-1}. In our previous study of 18C6-C_1OC_6 in aqueous solutions, the C–O stretching band of the M^+·18C6-C_1OC_6 complexes shifts to lower frequency compared to that of bare 18C6-C_1OC_6, and the IR intensity of the 18C6-C_1OC_6 part does not change so much upon complex formation.[10] As a result, their IR difference spectra show sigmoidal shapes, as seen in Fig. 2f.[10] Fig. 3 displays the model simulation of band contours in IR difference spectra. In this simulation, the IR bandwidth is assumed to be the same between bare CEs and metal ion–CE complexes, but the band position of the complexes is slightly shifted to lower frequency compared to the bare ones, and the IR difference spectra are obtained by subtracting the IR spectrum of the bare ones (Fig. 3b) from that of the complexes (Fig. 3a). Fig. 3c shows an IR difference spectrum with equal band intensity, providing a sigmoidal signal.[10] In Fig. 3d, the difference spectrum

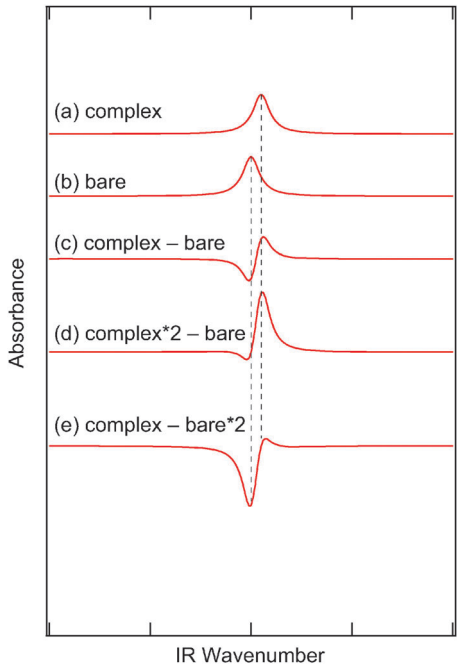

Fig. 3 The model simulation of band contours in IR difference spectra between CE complexes and bare CEs (see the text).

is obtained by assuming that the band intensity of the complexes is two times stronger than that of the bare ones. This gives a strong positive signal in the difference spectrum. This band shape well resembles that of the IR difference spectra for Li^+ and Na^+ in Fig. 2a and b. In Fig. 3e, we assume that the band intensity of the complexes is a half of that of the bare ones, showing a negative signal. This feature is similar to the spectra of the K^+, Rb^+ and Cs^+ complexes in Fig. 2c–e. Thus, all the spectral features in Fig. 2 can be attributed primarily to the IR intensity change of 15C5-C_1OC_6 upon complex formation.

We examine the dependence of the IR signal intensity on the concentration of MCl in aqueous solutions to obtain the equilibrium constant for the complex formation between M^+ and 15C5-C_1OC_6. Fig. 4 shows the plot of the IR difference intensity at around 1100 cm^{-1} in Fig. 2 as a function of the concentration of MCl. The data are fitted by Hill equations (solid curves), and the apparent dissociation constant (K_D) of the M^+·15C5-C_1OC_6 complexes is obtained.[11b] The curves in Fig. 4 show a noticeable difference between the metal ions. The titration curve of the Na^+ complex (Fig. 4b) shows the smallest K_D value ($\sim 2.8 \times 10^{-5}$ M) among the alkali metal ion complexes in Fig. 4. The data points of the Na^+ complex are highly scattered at the concentration more than 10^{-2} M; this is due to distorted band shapes in the spectra of the Na^+ complex at higher concentration (see Fig. 2b). One possibility for the distorted band contour is that the Na^+ ion may form 2 : 1 or higher complexes with 15C5 at higher concentration, changing the band shapes. The reciprocal of K_D (K_D^{-1}) gives the equilibrium constant for the complex formation. The values of K_D^{-1} for M^+·15C5-C_1OC_6 in aqueous solutions are plotted in Fig. 5a (blue circles), which are compared with those for M^+·18C6-C_1OC_6

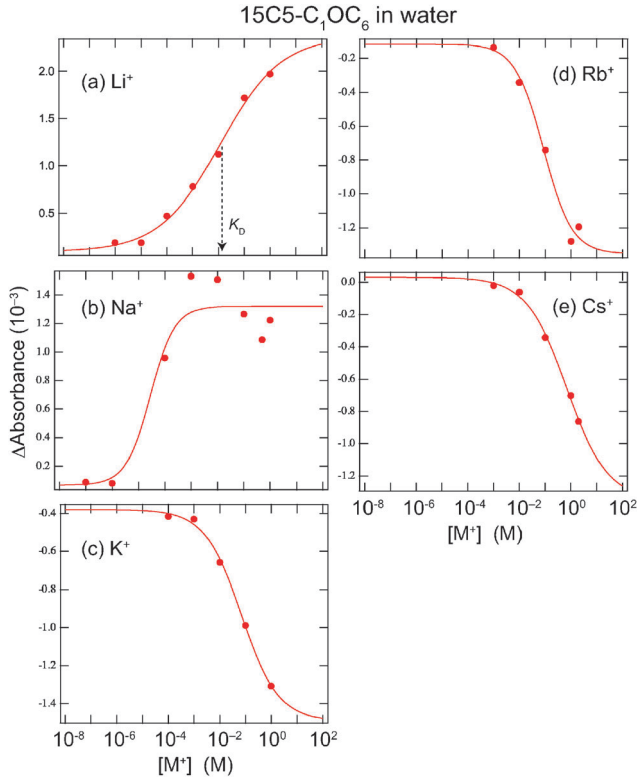

Fig. 4 The peak-to-peak amplitude at $\sim$1100 cm^{-1} in the IR difference spectra of the M^+·15C5-C_1OC_6 (M = Li, Na, K, Rb, and Cs) complexes (Fig. 2) as a function of the concentration of the M^+ ions in water (closed circles). The data are reproduced by Hill equations (solid curves).

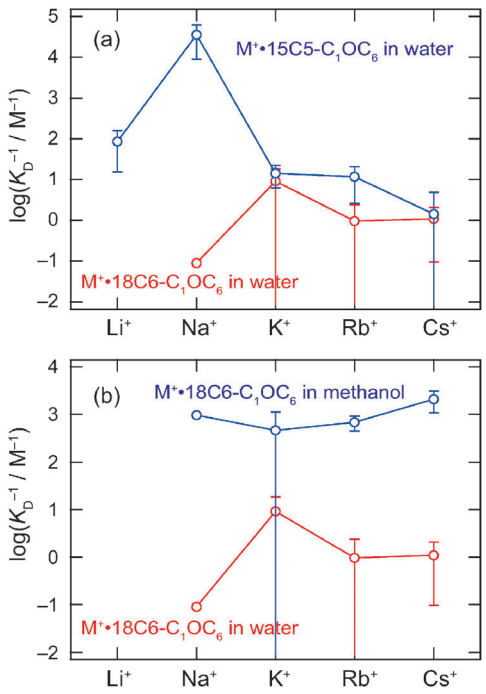

Fig. 5 The reciprocal of the apparent K_D values determined by fitting the intensity at around 1100 cm^{-1} in the IR difference spectra of (a) M^+·15C5-C_1OC_6 in water and (b) M^+·18C6-C_1OC_6 in methanol (blue circles). For comparison, the data of M^+·18C6-C_1OC_6 in water are shown in both panels (red circles) (ref. 10).

(red circles) obtained in our previous study.[10] The K_D^{-1} value of Na^+·15C5-C_1OC_6 is more than two orders of magnitude larger than those of the Li^+, K^+, Rb^+, and Cs^+ complexes, indicating the preference of Na^+ for the encapsulation by 15C5, which is in good contrast to the K^+ preference by 18C6.[10]

The optimized (the most stable) structures of bare 15C5-C_1OC_6-CH_3 and the M^+·15C5-C_1OC_6-CH_3 complexes are shown in Fig. 6. In the case of the Li^+ and Na^+ complexes, the metal ions are located in the 15C5 cavity. For the K^+, Rb^+, and Cs^+ complexes, the ions are too large to enter the 15C5 cavity. The C–O–C parts of the crown rings tend to orient the oxygen atoms to the metal ions. The C–O–C frames of the Li^+ and Na^+ complexes form a planar-like configuration with the metal ions. For the K^+, Rb^+, and Cs^+ complexes, since the metal ions are not in the center of the cavity but on it, the C–O–C frames show more bumpy features. Fig. 7 displays the calculated IR spectra of bare 15C5-C_1OC_6-CH_3 and the M^+·15C5-C_1OC_6-CH_3 complexes in the 1000–1500 cm^{-1} region. A scaling factor of 0.9389 is employed for the calculated vibrational frequencies, and the solid curves are the IR spectra reproduced by providing a Lorentzian component with a FWHM of 10 cm^{-1} to each vibration.[10] The IR spectrum of bare 15C5-C_1OC_6-CH_3 (Fig. 7a) has a maximum intensity of the C–O stretching vibrations at 1122 cm^{-1}, and it shifts to lower frequency with Li^+ ions (1108 cm^{-1}). The maximum position shifts further to lower frequency for Na^+ ions (1103 cm^{-1}), and then it is located closer to the position of bare species for K^+ at 1112 cm^{-1}, Rb^+ at 1115 cm^{-1}, and Cs^+ at 1118 cm^{-1}. The red shift of the C–O stretching vibration upon the complex formation was observed also for other CEs.[9a,l,10] By using the calculated IR spectra, we obtain the IR difference spectra (Fig. 8). For the production of the IR difference spectra of the Li^+ and Na^+ complexes, the calculated IR intensity of the complexes is multiplied by 2 before the subtraction. For the K^+, Rb^+, and Cs^+ spectra, on the other hand, the IR intensity of bare 15C5-C_1OC_6-CH_3 is multiplied by 2. These simulated spectra in Fig. 8 well reproduce the spectral features of the observed ones (Fig. 2). In the simulated difference spectra of Li^+ and Na^+ (Fig. 8a and b), a positive band emerge at around 1106 cm^{-1}, whereas the difference spectra of K^+, Rb^+, and Cs^+ (Fig. 8c–e) show a negative signal at ~1123 cm^{-1}, rather than a positive one like the Li^+ and Na^+ complexes. It should be noted again

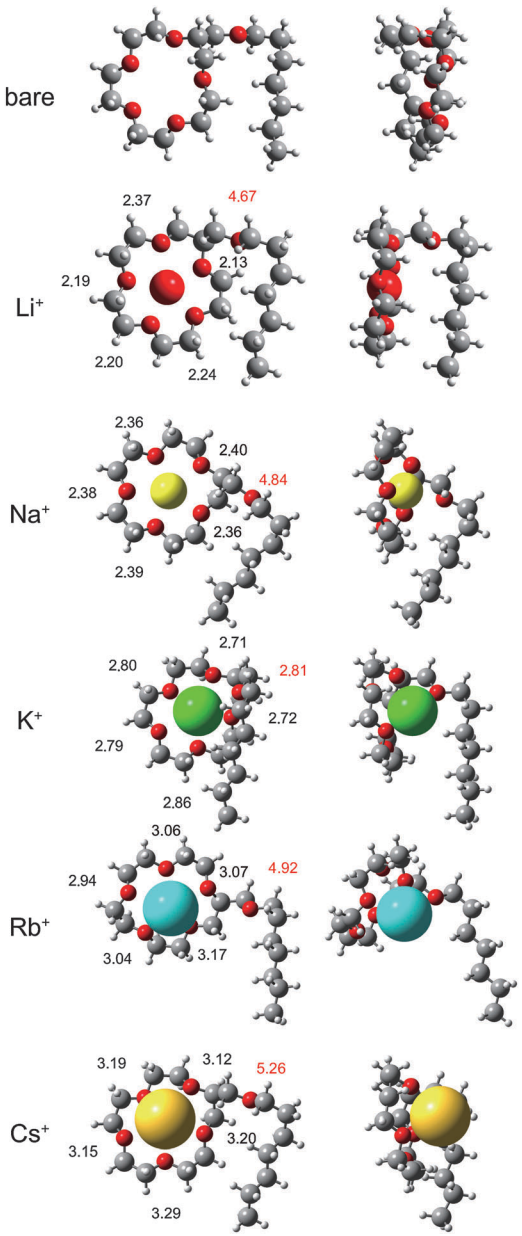

Fig. 6 The optimized structure of bare 15C5-C_1OC_6-CH_3 and the M^+·15C5-C_1OC_6-CH_3 complexes. The numbers in the figure show the $M^+\cdots O$ distance (Å).

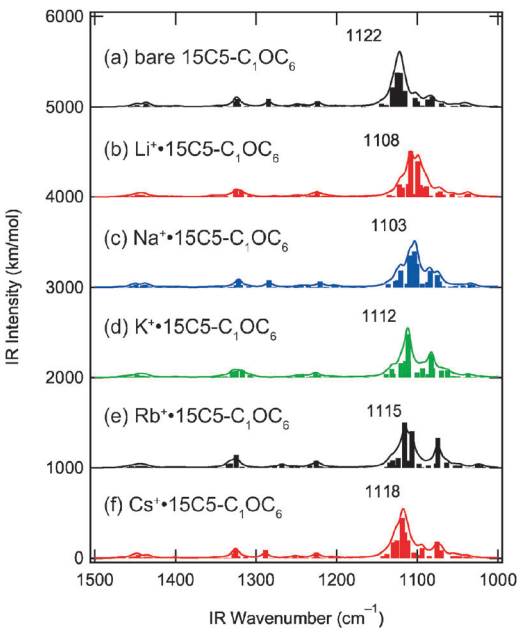

Fig. 7 The IR spectra of the M^+·15C5-C_1OC_6-CH_3 (M = Li, Na, K, Rb, and Cs) complexes and bare 15C5-C_1OC_6-CH_3 calculated at the M05-2X/6-31+G(d) level with the PCM of water. A scaling factor of 0.9389 is employed for the calculated vibrational frequencies. The solid curves are the IR spectra produced by providing a Lorentzian component with a FWHM of 10 cm^{-1} to each band.

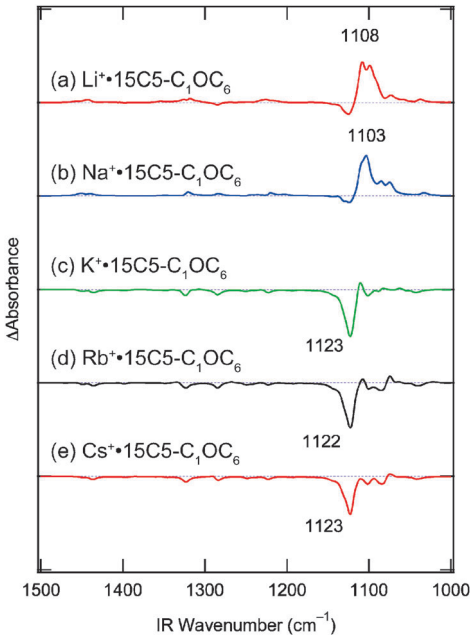

Fig. 8 The IR difference spectra made by subtracting the simulated IR spectrum of bare 15C5-C_1OC_6-CH_3 in Fig. 7a from those of the M^+·15C5-C_1OC_6-CH_3 complexes in Fig. 7b–f. In the simulation of the Li^+ and Na^+ complexes, the calculated IR intensity of the M^+·15C5-C_1OC_6-CH_3 complexes is multiplied by 2 before the subtraction, while for the K^+, Rb^+, and Cs^+ spectra, the IR intensity of bare 15C5-C_1OC_6-CH_3 is multiplied by 2 (see the text).

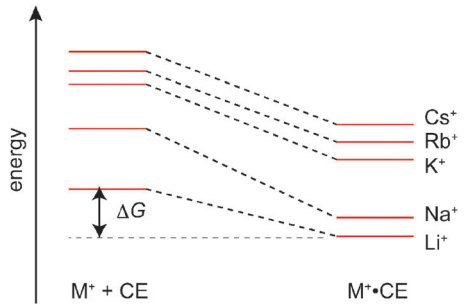

Fig. 9 Energy diagram proposed for the M^+·15C5-C_1OC_6 complexes in water.

that the main origin of the difference in the spectral features of the M^+·15C5-C_1OC_6 complexes (positive signals for Li^+ and Na^+ and negative ones for K^+, Rb^+, and Cs^+, Fig. 2a–e) is the difference of the relative IR intensity between the metal ion complexes and bare ones. As mentioned above, the calculated IR intensity for the M^+·15C5-C_1OC_6 complexes in Fig. 7 cannot be used as it is for the reproduction of the IR difference spectra in Fig. 2 or 8. The discrepancy in the IR intensity calculated and observed can be explained by the orientation of the 15C5 frame against the gold surfaces after the inclusion of the metal ions. As seen in Fig. 6, the K^+, Rb^+, and Cs^+ ions are displaced largely from the 15C5 cavity and likely to be exposed to the water phase more than the Li^+ and Na^+ ions. As a result, the M^+·15C5 part in the K^+, Rb^+, and Cs^+ complexes can take an orientation almost parallel to the water phase, or the gold surfaces, as drawn in Fig. S2a of the ESI.† For the M^+·15C5-C_1OC_6 complexes, the dipole derivatives of the C–O stretching vibrations are almost parallel to the 15C5 cavity (Fig. S2b and c of the ESI†). Osawa and coworkers demonstrated that in SEIRA spectroscopy a vibrational mode with its dipole derivative perpendicular to the gold surface is preferentially enhanced.[11c] Hence, the C–O stretching vibration of the M^+·15C5-C_1OC_6 (M = K, Rb, and Cs) complexes is less enhanced due to the parallel orientation, resulting in weaker IR intensity. The origin of the more enhanced nature of the Li^+ and Na^+ complexes is not clear at the present stage, but probably the M^+·15C5 part can take a perpendicular orientation to the gold surface with Li^+ and Na^+, due to the repulsive force between the neighboring complexes.

We then return to the results in Fig. 2 and 5a. The IR spectral features reflect the strength of the interaction between the metal ions and the crown ether in the complexes. From the similarity of the IR spectra in Fig. 2, the Li^+ and Na^+ ions undergo comparable interaction with 15C5-C_1OC_6, and the interaction in the K^+, Rb^+, and Cs^+ complexes is similar to each other and should be weaker than that in the Li^+ and Na^+ complexes. On the other hand, the equilibrium constant determined from the IR signal intensity shows clear preference for Na^+ over the other metal ions. From these findings, we can attribute the ion selectivity of Na^+ by 15C5-C_1OC_6 to the energy before and after complex formation. Fig. 9 shows the schematic energy diagram proposed for the M^+·15C5-C_1OC_6 complexes in water. The left side of Fig. 9 shows the energy levels of free ions and 15C5-C_1OC_6 in water, which are drawn on the basis of reported hydration molar free energy of alkali metal ions: −124.0 (Li^+), −100.1 (Na^+), −82.5 (K^+), −77.4 (Rb^+), −69.7 (Cs^+) kcal mol^{-1}.[16] Our IR spectra probe the complex structure or the strength of the interaction in M^+·15C5-C_1OC_6 on the right side of Fig. 9. The spectral resemblance in Fig. 2 indicates that the interaction energy between M^+ and 15C5-C_1OC_6 is similar for Li^+ and Na^+, and for K^+, Rb^+, and Cs^+, which is illustrated on the right side of Fig. 9. The equilibrium constant for the complex formation is governed by the difference in free energy (ΔG). The observed preference of Na^+ over K^+, Rb^+, and Cs^+ can be attributed to the strength of the interaction or the size matching in size between the metal ions and 15C5-C_1OC_6 (the right side of Fig. 9). In contrast, higher selectivity for Na^+ over Li^+ ions is attributed to the difference of solvation energy in aqueous solution between Na^+ and Li^+ (the left side of Fig. 9).[9h,m]

3.2. M^+·18C6 in water and methanol: solvent dependence

In our previous study, we reported the IR difference spectra of the M^+·18C6-C_1OC_6 complexes using aqueous solutions.[10] In this study, we perform the same experiment by using methanol solution to examine the solvent effect on the preference of the ion encapsulation. Fig. 10 displays the IR difference spectra of M^+·18C6-C_1OC_6 tagged on the gold surfaces with methanol solutions of MCl (M = Li, Na, K, Rb, and Cs). The concentration of MCl in methanol ranges from 10^{-5} to 10^{-2} M, and the blue curve in each panel of Fig. 9 corresponds to the spectrum with 10^{-2} M. No strong signal is observed in the spectra of the Li^+ complex (Fig. 10a), suggesting that the Li^+·18C6-C_1OC_6 complex

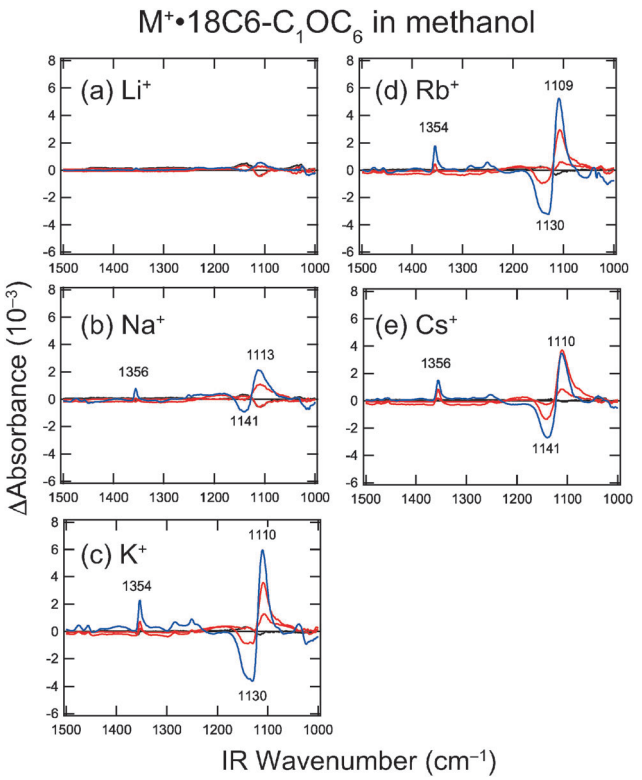

Fig. 10 The IR difference spectra of the M^+·18C6-C_1OC_6 (M = Li, Na, K, Rb, and Cs) complexes on the gold surface using MCl methanol solutions. The concentration of the MCl salts in methanol ranges from 10^{-5} to 10^{-2} M. The blue curves are the IR difference spectra measured at 10^{-2} M.

is hardly formed in this experiment. The Na^+ complex shows weak signals at around 1100 cm^{-1} (Fig. 10b). The amplitude of the signal is much stronger for the K^+, Rb^+, and Cs^+ complexes (Fig. 10c–e). The trend of the signal intensity in Fig. 10 is quite similar to that observed by using aqueous MCl solutions.[10] Hence, the interaction between M^+ and 18C6-C_1OC_6 in the M^+·18C6-C_1OC_6 complexes seems to be similar in methanol and in water. On the other hand, a noticeable difference between methanol and water solutions is seen for the absolute value of K_D^{-1} and ion selectivity. Fig. 5b shows the equilibrium constant of the M^+·18C6-C_1OC_6 complexes in methanol (blue circles) determined in this study; for comparison, the results in water are also displayed in the same figure (red circles).[10] The titration curves for obtaining K_D^{-1} of the M^+·18C6-C_1OC_6 complexes in methanol are shown in Fig. S3 of the ESI.† As described above, the results of the M^+·18C6-C_1OC_6 complexes in water show the maximum at K^+ ions, indicating the K^+ preference of 18C6. However, in methanol, we cannot find the preference for any specific ion. The equilibrium constants in methanol are almost the same for Na^+ to Cs^+, and these are much higher than those in water. This result suggests that the ion selectivity is strongly governed by the solvent effect, probably by less stability of free ions in methanol (less solvation energy) than in water. From the similarity of the IR spectra of M^+·18C6-C_1OC_6 between in methanol and water, the relative stability of M^+·18C6-C_1OC_6 in water for alkali metal ions is almost retained in methanol. Since the solvation energy in methanol is smaller than that in water, the energy levels of free ions will be lifted up in methanol compared to those in water.[17] As a result, the equilibrium constant for the complex formation becomes much bigger in methanol than that in water and loses the selectivity in methanol.

4. Conclusions

In this study, we synthesized thiol derivatives of 15-crown-5 and 18-crown-6 [2-(6-mercaptohexyloxy)methyl-15-crown-5 (15C5-C_1OC_6-SH) and 2-(6-mercaptohexyloxy)methyl-18-crown-6 (18C6-C_1OC_6-SH)], which are adsorbed on gold surfaces through S–Au bonds. The IR difference spectra of the M^+·15C5-C_1OC_6 complexes were observed using aqueous solutions of MCl by surface-enhanced infrared absorption (SEIRA) spectroscopy. The spectra in the 900–1500 cm^{-1} region show noticeable signals at around 1100 cm^{-1}, which correspond to the C–O stretching vibration. The spectral features suggest that the interaction between the metal ions and 15C5-C_1OC_6 is similar for Li^+ and Na^+ and for K^+, Rb^+, and Cs^+, and it changes drastically between Na^+ and K^+. On the other hand, the results of the equilibrium constant for the complex formation, which were obtained by the signal intensity of the IR difference spectra, show clear preference for Na^+ ions. We observed the IR difference spectra of M^+·18C6-C_1OC_6 in methanol and compared the results with those in water. The spectral patterns in methanol are almost the same as those in water. However, the equilibrium constant in methanol does not show clear preference for any metal ion, different from the K^+ preference in water. Hence, the ion selectivity of crown ethers is governed by a delicate balance between the intermolecular interaction between the host and guest species and the solvation energy of free ions in solution. This study suggests that the IR spectra measured by SEIRA spectroscopy are quite sensitive to the intermolecular interaction, the structure, and the orientation against the gold surface of host–guest complexes, but the evidence for guest selectivity emerges in the intensity of the spectra, rather than band positions or spectral patterns.

Acknowledgements

YI thanks the support from the Institute for Molecular Science through the Joint Studies Program (2012-2013). TE acknowledges Japan Society for the Promotion of Science (JSPS) for the support through a Grand-in-Aid project (25410017). The authors thank Mr Masaki Aoyama, Mr Nobuo Mizutani, and Ms Noriko Takada at Equipment Development Center in the Institute for Molecular Science for fabricating a Teflon chamber for SEIRA spectroscopy. This work was partly supported by grants from JSPS to YF (22247024 and 24650203).

References

1 (*a*) C. J. Pedersen, *J. Am. Chem. Soc.*, 1967, **89**, 7017–7036; (*b*) R. M. Izatt, J. S. Bradshaw, S. A. Nielsen, J. D. Lamb and J. J. Christensen, *Chem. Rev.*, 1985, **85**, 271–339; (*c*) R. M. Izatt, R. E. Terry, B. L. Haymore, L. D. Hansen, N. K. Dalley, A. G. Avondet and J. J. Christensen, *J. Am. Chem. Soc.*, 1976,

98, 7620–7626; (*d*) A. V. Bajaj and N. S. Poonia, *Coord. Chem. Rev.*, 1988, **87**, 55–213.

2 C. J. Pedersen, *Science*, 1988, **241**, 536–540.

3 F. H. Allen, *Acta Crystallogr., Sect. B: Struct. Sci.*, 2002, **58**, 380–388.

4 (*a*) M. B. More, D. Ray and P. B. Armentrout, *J. Am. Chem. Soc.*, 1998, **121**, 417–423; (*b*) B. P. Hay, J. R. Rustad and C. J. Hostetler, *J. Am. Chem. Soc.*, 1993, **115**, 11158–11164; (*c*) L. X. Dang, *J. Am. Chem. Soc.*, 1995, **117**, 6954–6960; (*d*) E. D. Glendening, D. Feller and M. A. Thompson, *J. Am. Chem. Soc.*, 1994, **116**, 10657–10669; (*e*) C. M. Choi, H. J. Kim, J. H. Lee, W. J. Shin, T. O. Yoon, N. J. Kim and J. Heo, *J. Phys. Chem. A*, 2009, **113**, 8343–8350; (*f*) D. Feller, M. A. Thompson and R. A. Kendall, *J. Phys. Chem. A*, 1997, **101**, 7292–7298; (*g*) S. E. Hill, D. Feller and E. D. Glendening, *J. Phys. Chem. A*, 1998, **102**, 3813–3819; (*h*) S. De, A. Boda and S. M. Ali, *THEOCHEM*, 2010, **941**, 90–101.

5 (*a*) Y. Inokuchi, O. V. Boyarkin, R. Kusaka, T. Haino, T. Ebata and T. R. Rizzo, *J. Am. Chem. Soc.*, 2011, **133**, 12256–12263; (*b*) Y. Inokuchi, O. V. Boyarkin, R. Kusaka, T. Haino, T. Ebata and T. R. Rizzo, *J. Phys. Chem. A*, 2012, **116**, 4057–4068; (*c*) Y. Inokuchi, R. Kusaka, T. Ebata, O. V. Boyarkin and T. R. Rizzo, *ChemPhysChem*, 2013, **14**, 649–660; (*d*) Y. Inokuchi, T. Ebata, T. R. Rizzo and O. V. Boyarkin, *J. Am. Chem. Soc.*, 2014, **136**, 1815–1824.

6 (*a*) T. E. Cooper, D. R. Carl, J. Oomens, J. D. Steill and P. B. Armentrout, *J. Phys. Chem. A*, 2011, **115**, 5408–5422; (*b*) F. Gamez, P. Hurtado, S. Hamad, B. Martinez-Haya, G. Berden and J. Oomens, *ChemPlusChem*, 2012, **77**, 118–123; (*c*) F. Gamez, P. Hurtado, B. Martinez-Haya, G. Berden and J. Oomens, *Int. J. Mass Spectrom.*, 2011, **308**, 217–224; (*d*) P. Hurtado, A. R. Hortal, F. Gámez, S. Hamad and B. Martínez-Haya, *Phys. Chem. Chem. Phys.*, 2010, **12**, 13752; (*e*) C. N. Stedwell, J. F. Galindo, K. Gulyuz, A. E. Roitberg and N. C. Polfer, *J. Phys. Chem. A*, 2013, **117**, 1181–1188; (*f*) J. D. Rodriguez and J. M. Lisy, *Int. J. Mass Spectrom.*, 2009, **283**, 135–139; (*g*) J. D. Rodriguez and J. M. Lisy, *J. Phys. Chem. A*, 2009, **113**, 6462–6467; (*h*) J. D. Rodriguez, T. D. Vaden and J. M. Lisy, *J. Am. Chem. Soc.*, 2009, **131**, 17277–17285; (*i*) J. D. Rodriguez, D. Kim, P. Tarakeshwar and J. M. Lisy, *J. Phys. Chem. A*, 2010, **114**, 1514–1520; (*j*) J. D. Rodriguez and J. M. Lisy, *J. Am. Chem. Soc.*, 2011, **133**, 11136–11146.

7 G. W. Buchanan, *Prog. Nucl. Magn. Reson. Spectrosc.*, 1999, **34**, 327–377.

8 M. R. Antonio, M. L. Dietz, M. P. Jensen, L. Soderholm and E. P. Horwitz, *Inorg. Chim. Acta*, 1997, **255**, 13–20.

9 (*a*) M. F. Belian, G. F. De Sa, S. Alves and R. F. De Farias, *J. Coord. Chem.*, 2007, **60**, 173–183; (*b*) B. Brzezinski, G. Schroeder, A. Rabold and G. Zundel, *J. Phys. Chem.*, 1995, **99**, 8519–8523; (*c*) M. De Backer, M. Hureau, M. Depriester, A. Deletoille, A. L. Sargent, P. B. Forshee and J. W. Sibert, *J. Electroanal. Chem.*, 2008, **612**, 97–104; (*d*) P. Firman, L. J. Rodriguez, S. Petrucci and E. M. Eyring, *J. Phys. Chem.*, 1992, **96**, 2376–2381; (*e*) B. Gierczyk, G. Schroeder, G. Wojciechowski, B. Rozalski, B. Brzezinski and G. Zundel, *Phys. Chem. Chem. Phys.*, 1999, **1**, 4897–4901; (*f*) L. J. Hilliard, M. R. Rice and H. S. Gold, *Spectrochim. Acta, Part A*, 1982, **38**, 611–615; (*g*) H. P. Hopkins and A. B. Norman, *J. Phys. Chem.*, 1980, **84**, 309–314; (*h*) D. Midgley, *Chem. Soc. Rev.*, 1975, **4**, 549–568; (*i*) N. S. Poonia, *J. Am. Chem. Soc.*, 1974, **96**, 1012–1019; (*j*) P. Przybylski, G. Schroeder, B. Brzezinski and F. Bartl, *J. Phys. Org. Chem.*, 2003, **16**, 289–297; (*k*) M. J. Tapia, A. J. M. Valente, H. D. Burrows, V. Calderon, F. Garcia and J. M. Garcia, *Eur. Polym. J.*, 2007, **43**, 3838–3848; (*l*) H. Temel, H. Hosgoren and M. Boybay, *Spectrosc. Lett.*, 2002, **35**, 1–8; (*m*) A. T. Tsatsas, R. W. Stearns and W. M. Risen, *J. Am. Chem. Soc.*, 1972, **94**, 5247–5253.

10 Y. Inokuchi, T. Mizuuchi, T. Ebata, T. Ikeda, T. Haino, T. Kimura, H. Guo and Y. Furutani, *Chem. Phys. Lett.*, 2014, **592**, 90–95.

11 (*a*) K. Ataka, F. Giess, W. Knoll, R. Naumann, S. Haber-Pohlmeier, B. Richter and J. Heberle, *J. Am. Chem. Soc.*, 2004, **126**, 16199–16206; (*b*) Y. Furutani, H. Shimizu, Y. Asai, T. Fukuda, S. Oiki and H. Kandori, *J. Phys. Chem. Lett.*, 2012, **3**, 3806–3810; (*c*) M. Osawa, *Bull. Chem. Soc. Jpn.*, 1997, **70**, 2861–2880; (*d*) Y. Furutani, H. Shimizu, Y. Asai, S. Oiki and H. Kandori, *Biophys. Physicobiol.*, 2015, **12**, 37–45.

12 (*a*) H. X. Chen, Y. S. Gal, S. H. Kim, H. J. Choi, M. C. Oh, J. Lee and K. Koh, *Sens. Actuators, B*, 2008, **133**, 577–581; (*b*) S. Flink, B. A. Boukamp, A. van den Berg, F. van Veggel and D. N. Reinhoudt, *J. Am. Chem. Soc.*, 1998, **120**, 4652–4657; (*c*) S. Flink, H. Schonherr, G. J. Vancso, F. A. J. Geurts, K. G. C. van Leerdam, F. van Veggel and D. N. Reinhoudt, *J. Chem. Soc., Perkin Trans. 2*, 2000, 2141–2146; (*d*) S. Flink, F. van Veggel and D. N. Reinhoudt, *J. Phys. Chem. B*, 1999, **103**, 6515–6520; (*e*) S. Flink, F. van Veggel and D. N. Reinhoudt, *Adv. Mater.*, 2000, **12**, 1315–1328.

13 H. Guo, T. Kimura and Y. Furutani, *Chem. Phys.*, 2013, **419**, 8–16.

14 (*a*) H. Goto and E. Osawa, *J. Am. Chem. Soc.*, 1989, **111**, 8950–8951; (*b*) H. Goto and E. Osawa, *J. Chem. Soc., Perkin Trans. 2*, 1993, 187–198.

15 M. J. Frisch, G. W. Trucks, H. B. Schlegel, G. E. Scuseria, M. A. Robb, J. R. Cheeseman, G. Scalmani, V. Barone, B. Mennucci, G. A. Petersson, H. Nakatsuji, M. Caricato, X. Li, H. P. Hratchian, A. F. Izmaylov, J. Bloino, G. Zheng, J. L. Sonnenberg, M. Hada, M. Ehara, K. Toyota, R. Fukuda, J. Hasegawa, M. Ishida, T. Nakajima, Y. Honda, O. Kitao, H. Nakai, T. Vreven, J. Montgomery, Jr., J. E. Peralta, F. Ogliaro, M. Bearpark, J. J. Heyd, E. Brothers, K. N. Kudin, V. N. Staroverov, R. Kobayashi, J. Normand, K. Raghavachari, A. Rendell, J. C. Burant, S. S. Iyengar, J. Tomasi, M. Cossi, N. Rega, N. J. Millam, M. Klene, J. E. Knox, J. B. Cross, V. Bakken, C. Adamo, J. Jaramillo, R. Gomperts, R. E. Stratmann, O. Yazyev, A. J. Austin, R. Cammi, C. Pomelli, J. W. Ochterski, R. L. Martin, K. Morokuma, V. G. Zakrzewski, G. A. Voth, P. Salvador, J. J. Dannenberg, S. Dapprich, A. D. Daniels, Ö. Farkas, J. B. Foresman, J. V. Ortiz, J. Cioslowski and D. J. Fox, *Gaussian 09, Revision A.1*, Gaussian, Inc., Wallingford CT, 2009.

16 J. Carlsson and J. Åqvist, *J. Phys. Chem. B*, 2009, **113**, 10255–10260.

17 J. R. Bontha and P. N. Pintauro, *J. Phys. Chem.*, 1992, **96**, 7778–7782.